J. KSIAM Vol.16, No.4, 225–234, 2012

HIGH-ORDER POTENTIAL FLOW MODELS FOR HYDRODYNAMIC UNSTABLE INTERFACE

SUNG-IK SOHN

DEPARTMENT OF MATHEMATICS, GANGNEUNG-WONJU NATIONAL UNIVERSITY, GANGNEUNG, KOREA
E-mail address: sohnsi@gwnu.ac.kr

ABSTRACT. We present two high-order potential flow models for the evolution of the interface in the Rayleigh-Taylor instability in two dimensions. One is the source-flow model and the other is the Layzer-type model which is based on an analytic potential. The late-time asymptotic solution of the source-flow model for arbitrary density jump is obtained. The asymptotic bubble curvature is found to be independent to the density jump of the fluids. We also give the time-evolution solutions of the two models by integrating equations numerically. We show that the two high-order models give more accurate solutions for the bubble evolution than their low-order models, but the solution of the source-flow model agrees much better with the numerical solution than the Layzer model.

1. INTRODUCTION

Fluid mixing occurs frequently in basic science and engineering applications. When a heavy fluid is supported by a lighter fluid in a gravitational field, the interface between the fluids is unstable under small disturbances. This phenomenon is known as the Rayleigh-Taylor (RT) instability [1, 2]. The RT instability may occur whenever the density and pressure gradients are in opposite directions and plays important roles in many fields ranging from astrophysics to inertial confinement fusion [3]. To investigate dynamics of this instability, extensive researches have been conducted for last decades. For a review, see Sharp [3].

Small perturbations at the interface in the RT instability grow into nonlinear structures in the form of bubbles and spikes. (See Fig. 1.) A bubble (spike) is a portion of the light (heavy) fluid penetrating into the heavy (light) fluid. At late times, the bubble in the RT instability attains a constant velocity. Eventually, turbulent mixing caused by vortex structures around spikes breaks the ordered fluid motion.

The main purpose of this paper is to develop high-order models for the interface evolution in the single-mode RT instability. Theoretical models for comprehensive descriptions of the motion of the interface are the potential flow models proposed by Layzer [4] and Zufiria [5]. Both the Layzer and Zufiria models approximate the shape of the interface near the bubble (or

Received by the editors April 30 2012; Accepted October 5 2012.
2010 *Mathematics Subject Classification.* 76B07, 76E17.
Key words and phrases. Rayleigh-Taylor instability, potential-flow models, bubble evolution.

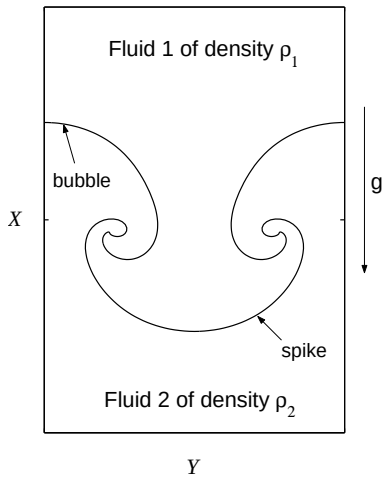

FIGURE 1. Flow description of RT instability. g represents the gravitational acceleration, and $\rho_1 > \rho_2$.

spike) tip as a parabola and give a set of ordinary differential equations to determine the position, velocity and curvature of the bubble (or spike). The main difference of the two models is that the velocity potential in the Layzer model is an analytical function of sinusoidal form, while in the Zufiria model, it has a point source (singularity). The Layzer and Zufiria models were limited to the case of infinite density ratio (fluid/vacuum) for a long time [6], but in the last decade there have been significant progresses in the models. Goncharov [7] and Sohn [8] generalized the Layzer model and the Zufiria model to the system of finite density jumps for the interface, respectively. Sohn [9, 10] also applied the Zufiria model to the multiple bubble interaction, and recently succeeded in the extension of the Layzer model to the unstable interfaces with surface tension and viscosity. Cao et al. [11] reported viscosity effects on the RT instability, by using the Zufiria model.

The potential flow models gave good predictions for the bubble velocity, but there were relatively large differences in the bubble curvature between the solutions of the models and numerical results. Moreover, the issue of the dependence of the bubble curvature on the density jump is not fully discovered yet. The bubble curvature is an important parameter because it sets a length scale and plays a key role in the dynamics of the bubble merger in the evolution of the initial multi-mode interface [9, 12]. In this paper, we present high-order solutions of the source-flow (Zufiria) model and the Layzer model to give quantitatively correct predictions for the bubble evolution.

In Section 2, we describe the high-order source-flow model for the motion of the interface of arbitrary density jump, and in Section 3, give the asymptotic solution of the bubble from the source-flow model. In Section 4, we present the high-order Layzer-model for the interface of infinite density ratio. Section 5 gives the time-evolution solutions of the bubble from the two high-order models, in comparisons with numerical results. Section 6 gives conclusions.

2. HIGH-ORDER SOURCE-FLOW MODEL

We consider an interface in a vertical channel filled with two fluids of different densities in two dimensions. The fluids are assumed as incompressible and inviscid. The densities of the upper (heavy) and lower (light) fluid are denoted as ρ_1 and ρ_2, respectively. From the assumption of the potential flow, there exist complex potentials $W_1(z) = \phi_1 + i\psi_1$ for the upper fluid and $W_2(z) = \phi_2 + i\psi_2$ for the lower fluid, where ϕ is the velocity potential and ψ the stream function. In the laboratory frame of reference, the location of the bubble tip is $Z(t) = X(t) + i\,Y(t)$ with $Y(t) = L/2$, where L is the channel width. The bubble moves in the x-direction with the tip velocity U. It is convenient to choose a frame of reference $(\hat{x}, \hat{y})$ moving together with the tip of the bubble. In other words, the frame of reference moves with the bubble velocity U. In this moving frame, the location of the bubble tip is $\hat{x} = \hat{y} = 0$ and the interface in the vicinity of the bubble tip can be written as

$$\eta(\hat{x}, \hat{y}, t) = \hat{x} + \sum_{j=1}^{\infty} \zeta_j(t)\, \hat{y}^{2j} = 0, \tag{2.1}$$

assuming the symmetry of the bubble. We here take the approximation of the interface (2.1) up to fourth-order in $\hat{y}$. The bubble curvature is denoted as $\xi = 2\zeta_1$.

The evolution of the bubble is determined by the kinematic condition and the Bernoulli equation

$$\frac{D\eta(\hat{x}, \hat{y}, t)}{Dt} = u + \sum_{j=1}^{\infty} \left(\frac{d\zeta_j}{dt} \hat{y}^{2j} + 2j\, \zeta_j\, \hat{y}^{2j-1} v \right) = 0, \tag{2.2}$$

$$\rho_1 \left[\frac{\partial \phi_1}{\partial t} + \frac{1}{2} |\nabla \phi_1|^2 + \left(g + \frac{dU}{dt} \right) \hat{x} \right] = \rho_2 \left[\frac{\partial \phi_2}{\partial t} + \frac{1}{2} |\nabla \phi_2|^2 + \left(g + \frac{dU}{dt} \right) \hat{x} \right], \tag{2.3}$$

where u and v are $\hat{x}$ and $\hat{y}$ components of the interface velocity, and g is the gravitational acceleration. The kinematic condition implies the continuity of the normal component of the fluid velocity across the interface.

The complex potentials of the fluids in the source-flow model [8, 9] are taken as

$$W_1(\hat{z}) = Q_1 \log \left[1 - e^{-k(\hat{z}+H)} \right] - U\hat{z}, \tag{2.4}$$

$$W_2(\hat{z}) = Q_2 \log \left[1 - e^{-k(\hat{z}-H)} \right] + (K - U)\hat{z}, \tag{2.5}$$

where $k = 2\pi/L$ is the wave number. Expanding the potentials (2.4) and (2.5) in powers of $\hat{z}$, and using the relation $dW_i/d\hat{z} = u - iv,\ i = 1, 2$, one can obtain the expressions for the interface velocity taken from the upper and lower fluids. Substituting these expressions into the kinematic condition (2.2), and satisfying up to the fourth-order in $\hat{y}$, we have

$$U = c_1 Q_1 = \tilde{c}_1 Q_2 + K, \tag{2.6}$$

$$\frac{d\zeta_1}{dt} = Q_1 \left(3c_2\zeta_1 + \frac{c_3}{2} \right) = Q_2 \left(3\tilde{c}_2\zeta_1 + \frac{\tilde{c}_3}{2} \right), \tag{2.7}$$

$$\frac{d\zeta_2}{dt} = Q_1\left(5c_2\zeta_2 - \frac{5}{2}c_3\zeta_1^2 - \frac{5}{6}c_4\zeta_1 - \frac{c_5}{24}\right)$$
$$= Q_2\left(5\tilde{c}_2\zeta_2 - \frac{5}{2}\tilde{c}_3\zeta_1^2 - \frac{5}{6}\tilde{c}_4\zeta_1 - \frac{\tilde{c}_5}{24}\right). \quad (2.8)$$

The second and fourth order equations in $\hat{y}$ of Eq. (2.3) are

$$\left(c_1\zeta_1 + \frac{c_2}{2}\right)\frac{dQ_1}{dt} + Q_1\left(c_2\zeta_1 + \frac{c_3}{2}\right)\frac{dH}{dt} - \frac{1}{2}Q_1^2c_2^2 + g\zeta_1$$
$$= r\left[\left(\tilde{c}_1\zeta_1 + \frac{\tilde{c}_2}{2}\right)\frac{dQ_2}{dt} + \frac{dK}{dt} - Q_2\left(\tilde{c}_2\zeta_1 + \frac{\tilde{c}_3}{2}\right)\frac{dH}{dt} - \frac{1}{2}Q_2^2\tilde{c}_2^2 + g\zeta_1\right], \quad (2.9)$$

$$\left(\frac{c_2}{2}\zeta_1^2 + \frac{c_3}{2}\zeta_1 + \frac{c_4}{24} - c_1\zeta_2\right)\frac{dQ_1}{dt} + Q_1\left(\frac{c_3}{2}\zeta_1^2 + \frac{c_4}{2}\zeta_1 + \frac{c_5}{24} - c_2\zeta_2\right)\frac{dH}{dt} + G_1$$
$$= r\left[\left(\frac{\tilde{c}_2}{2}\zeta_1^2 + \frac{\tilde{c}_3}{2}\zeta_1 + \frac{\tilde{c}_4}{24} - \tilde{c}_1\zeta_2\right)\frac{dQ_2}{dt}\right.$$
$$\left. -Q_2\left(\frac{\tilde{c}_3}{2}\zeta_1^2 + \frac{\tilde{c}_4}{2}\zeta_1 + \frac{\tilde{c}_5}{24} - \tilde{c}_2\zeta_2\right)\frac{dH}{dt} + G_2\right], \quad (2.10)$$

where

$$G_1 = \frac{Q_1^2}{2}\left(c_2^2\zeta_1^2 - 2c_2c_3\zeta_1 + \frac{c_3^2}{4} - \frac{c_2c_4}{3}\right) + g\zeta_2,$$
$$G_2 = \frac{Q_2^2}{2}\left(\tilde{c}_2^2\zeta_1^2 - 2\tilde{c}_2\tilde{c}_3\zeta_1 + \frac{\tilde{c}_3^2}{4} - \frac{\tilde{c}_2\tilde{c}_4}{3}\right) + g\zeta_2,$$

and $r = \rho_2/\rho_1$ denotes the density ratio. Here, the expressions for c_i are

$$c_1 = \frac{k}{e^{kH}-1}, \qquad c_2 = -\frac{k^2e^{kH}}{(e^{kH}-1)^2}, \qquad c_3 = \frac{k^3e^{kH}(e^{kH}+1)}{(e^{kH}-1)^3},$$
$$c_4 = -\frac{k^4e^{kH}(e^{2kH}+4e^{kH}+1)}{(e^{kH}-1)^4}, \qquad c_5 = \frac{k^5e^{kH}(e^{3kH}+11e^{2kH}+11e^{kH}+1)}{(e^{kH}-1)^5}.$$

and $\tilde{c}_i(H) = c_i(-H)$. Equations (2.6)-(2.10) determine the dynamics of the bubble of finite density contrast. Note that Eq. (2.8) is a new equation from the low order model [8], and Eqs. (2.6)-(2.10) are the same as the low order model, except the terms with ζ_2 in Eq. (2.10).

One can check that Eqs. (2.6)-(2.10) remain the same even after retaining higher-order terms than the fourth order in $\hat{y}$, and thus expansions higher than the fourth order are not needed in this model. Usually, in other models, including the Layzer model, a higher-order expansion contributes a corresponding correction to the bubble motion. This is a crucial difference of the source-flow model from other theoretical models, and it explains why the high-order source-flow model is found to provide an accurate solution for the bubble motion.

3. ASYMPTOTIC SOLUTION OF SOURCE-FLOW MODEL

We now find the asymptotic solution for the bubble motion from the higher-order source-flow model. The system of the ordinary differential equations (2.6)-(2.10) has a critical point which corresponds to a steady rising bubble. The critical point (or, asymptotic solution) can be easily obtained by setting all the time derivatives of the variables to zero in Eqs. (2.7)-(2.10). The high-order asymptotic solution for the RT bubble is

$$\begin{aligned} &\zeta_1 \to \frac{k(\lambda+1)}{6(\lambda-1)}, && \zeta_2 \to \frac{k^3(\lambda^3+\lambda^2+\lambda+1)}{180(\lambda-1)^3}, \\ &H \to \frac{1}{k}\,\log\lambda, && Q_1 \to \sqrt{\frac{2(\lambda+1)(\lambda-1)^3 Ag}{3\,\lambda\,(1+A)k^3}}, \\ &U \to \frac{\sqrt{\lambda^2-1}}{\lambda}\sqrt{\frac{2Ag}{3(1+A)k}}, && Q_2 \to 0, \qquad K \to U. \end{aligned} \tag{3.1}$$

Here, A is the Atwood number, defined as $A = (\rho_1 - \rho_2)/(\rho_1 + \rho_2)$, and $\lambda = e^{kH(t\to\infty)} = (20 + 3\sqrt{39})/7$, which is the root, larger than 1, of the polynomial $p(\lambda) = 7\lambda^2 - 40\lambda + 7$. Therefore, from Eq. (3.1), the asymptotic bubble velocity is $0.984\sqrt{2Ag/(3(1+A)k)}$, and the asymptotic bubble curvature is $0.480k$, which is independent to the density jump. Note that the asymptotic solution of the low-order source-flow model [8] is $0.964\sqrt{2Ag/(3(1+A)k)}$ for the bubble velocity and $0.577k$ for the bubble curvature. Therefore, the correction factors of the high-order solution to the low-order solution are $U^{\rm high}/U^{\rm low} = 1.02$ for the velocity, and $\xi_1^{\rm high}/\xi_1^{\rm low} = 0.83$ for the curvature.

4. HIGH-ORDER LAYZER MODEL

We present the high-order Layzer model for the case of $A = 1$. For the Layzer model, we take the laboratory frame of reference. In this frame, the interface around the bubble tip can be approximated by

$$x = \eta(y,t) = \sum_{j=0}^{\infty} \zeta_j(t)\, y^{2j}. \tag{4.1}$$

Then, ζ_0 represents the longitudinal position of the bubble tip, and $d\zeta_0/dt$ is the velocity of the bubble tip. We give a general form of the velocity potential in the Layzer-type model by

$$\phi(x,y,t) = \sum_{\substack{j=1 \\ j:\ odd}}^{\infty} a_j(t)\ \cos(jky)\, e^{-jkx}. \tag{4.2}$$

The evolution of the bubble is again governed by the kinematic condition and the Bernoulli equation. In the case of $A = 1$, the right hand side of the Bernoulli equation (2.3) is set to zero.

One may apply the similar procedure as Section 2, to derive high-order equations. Satisfying the kinematic condition up to the fourth-order in y, we obtain the following equations

$$\frac{d\zeta_0}{dt} = -k \sum j a_j \, e^{-jk\zeta_0}, \tag{4.3}$$

$$\frac{d\zeta_1}{dt} = k^2 \sum j^2 \left(3\zeta_1 + \frac{1}{2} jk \right) a_j \, e^{-jk\zeta_0}, \tag{4.4}$$

$$\frac{d\zeta_2}{dt} = k^2 \sum j^2 \left(5\zeta_2 - \frac{5}{2} jk\zeta_1^2 - \frac{5}{6} j^2 k^2 \zeta_1 - \frac{1}{24} j^3 k^3 \right) a_j \, e^{-jk\zeta_0}, \tag{4.5}$$

where all the summations are taken for $j = 1$ and 3. The second and fourth order equations from the Bernoulli equation are given by

$$\begin{aligned} k \sum j \left(\zeta_1 + \frac{1}{2} jk \right) e^{-jk\zeta_0} \frac{da_j}{dt} &= \frac{1}{2} k^4 \left(\sum j^2 a_j e^{-jk\zeta_0} \right)^2 \\ &\quad -k^3 \left(\sum j a_j e^{-jk\zeta_0} \right) \left[\sum j^2 a_j \left(\zeta_1 + \frac{1}{2} jk \right) e^{-jk\zeta_0} \right] + g\zeta_1, \end{aligned} \tag{4.6}$$

$$\begin{aligned} & k \sum j \left(\zeta_2 - \frac{1}{2} jk\zeta_1^2 - \frac{1}{2} j^2 k^2 \zeta_1 - \frac{1}{24} j^3 k^3 \right) e^{-jk\zeta_0} \frac{da_j}{dt} \\ = \; & \frac{1}{2} k^4 \left[\sum j^2 \left(\zeta_1 + \frac{1}{2} jk \right) a_j e^{-jk\zeta_0} \right]^2 \\ & +k^3 \left(\sum j a_j e^{-jk\zeta_0} \right) \left[\sum j^2 \left(-\zeta_2 + \frac{1}{2} jk\zeta_1^2 + \frac{1}{2} j^2 k^2 \zeta_1 + \frac{1}{24} j^3 k^3 \right) a_j e^{-jk\zeta_0} \right] \\ & -k^5 \left(\sum j^2 a_j e^{-jk\zeta_0} \right) \left[\sum j^3 \left(\zeta_1 + \frac{1}{6} jk \right) a_j e^{-jk\zeta_0} \right]^2 + g\zeta_2. \end{aligned} \tag{4.7}$$

Equations (4.3)-(4.7) determine the evolution of the bubble of infinite density ratio. In fact, it is possible to develop a high-order Layzer model for the case of finite density jump, but we have found that the equations in that model are quite coupled, and it is difficult to solve them.

5. COMPARISONS OF THE MODELS

We now examine the agreement of the models by comparing the finite-time solutions of the models with numerical results, for two cases of the Atwood number. The time-evolution solution of the source-flow model can be obtained by solving Eqs. (2.6)-(2.10) numerically. Differentiating Eqs. (2.6) and (2.7), dQ_2/dt and dK/dt in Eqs. (2.9) and (2.10) can be expressed in terms of dQ_1/dt, dH/dt, and other variables, Then, Eqs. (2.9) and (2.10) become the ordinary differential equations of dQ_1/dt and dH/dt, so that they can be integrated. For numerical integrations, we employ the standard fourth-order Runge-Kutta method. On the

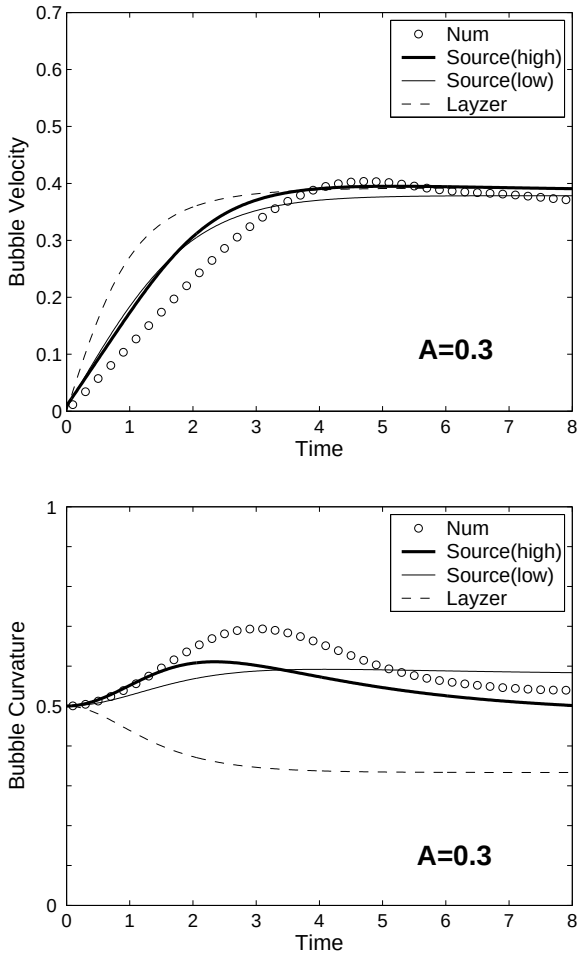

FIGURE 2. Bubble velocity and curvature for $A = 0.3$ from the low- and high-order source-flow models, the low-order Layzer model, and the numerical result.

other hand, the solution of the Layzer model can be obtained by integrating Eqs. (4.3)-(4.7) without any difficulty, because only da_1/dt and da_3/dt in Eqs. (4.6) and (4.7) are coupled.

In Figure 2, we compare the solutions for the bubble velocity and curvature of the RT instability for $A = 0.3$ from the low- and high-order source-flow model, and the low-order Layzer model [7] with the numerical result taken from Sohn [13]. The units in Fig. 2 (and also Fig. 3) are dimensionless. The dimensionless velocity, curvature and time are defined by $U\sqrt{k/g}$, ζ_1/k and $t\sqrt{kg}$, respectively. The numerical simulations in [13] are performed by the point vortex method based on the vortex sheet model. Note that the point vortex method has a regularization parameter for the finite density jump cases, which yields smoothing effects on

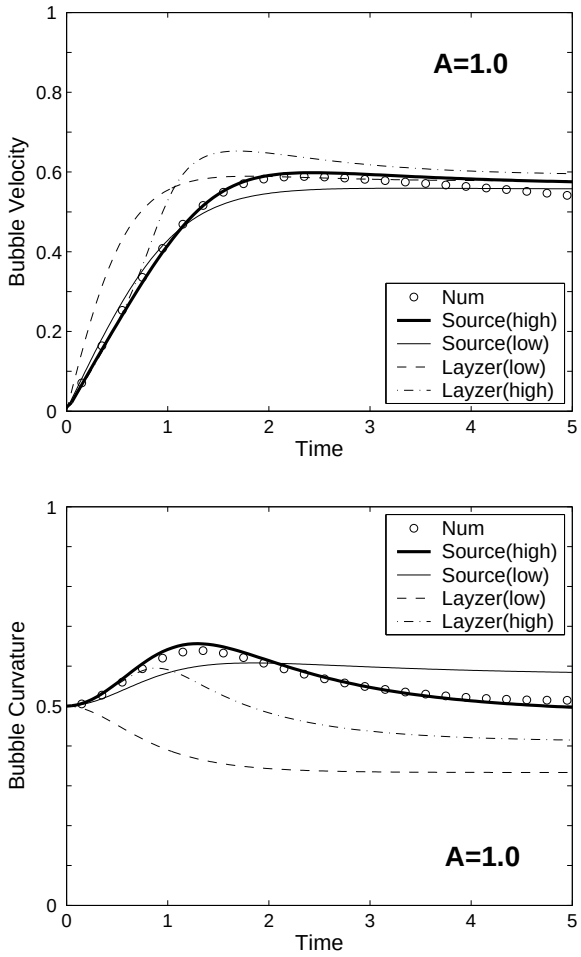

FIGURE 3. Bubble velocity and curvature for $A = 1$ from the low- and high-order source-flow models, the low- and high-order Layzer model, and the numerical result.

the solution. The physical parameters are set to $g = 1$ cm/s^2 and $k = 1$ cm^{-1}, and the initial amplitude of the interface is 0.5 cm. Figure 2 shows that the low-order source-flow model provides a good prediction for the bubble velocity, but not for the bubble curvature. The high-order solution of the source-flow model for the bubble curvature fits fairly well with the numerical solution. The growth of the bubble curvature at the early nonlinear stage is explained by the higher-order model. The Layzer model also gives a good prediction for the bubble velocity at the late time, but not at the early time. The bubble curvature from the Layzer model is quite different from the numerical result.

Figure 3 plots the solutions for the velocity and curvature of the RT bubble for $A = 1$ from the low- and high-order source-flow models, the low- and high-order Layzer models, and the numerical result. Figure 3 shows that the solution of the high-order source-flow model is in excellent agreements for both the bubble velocity and the curvature. This result indicates that the agreement of the source-flow model with the numerical result is better for larger density jump. We also find that for the bubble velocity, the solutions of the source-flow models again fit better than the Layzer models. The prediction for the bubble curvature from the low-order Layzer model is much improved by the higher-order model, but the difference with the numerical solution is still fairly large. This implies that some contributions from even higher-order variables are neglected in the model. To reduce the difference, equations higher than the fourth-order are required, but it is a formidable task.

6. CONCLUSIONS

We have presented the high-order solutions for the bubble evolution in the RT instability from the singular and analytic potential-flow models. The high-order source-flow model gives good predictions for both the bubble velocity and the curvature in the RT instability, over all times. The results presented in the paper validates that the source-type potential provides an appropriate description for the evolution of the unstable interface.

We have found the limitations of the Layzer model. In order to give quantitative predictions for the bubble, the Layzer model requires even higher-order expansions, while the present source-flow model has all the fourth-order contributions, We presented the high-order Layzer model only for the case of the infinite density ratio. Even if one finds a procedure of the numerical integration for the high-order Layzer model for the finite density jumps, it seems to be not promising.

The asymptotic bubble curvature of the RT instability is shown to be independent to the Atwood number. This behavior of the RT bubble is consistent with results of full numerical simulations for the Euler equation [14]. It is also contrasted with the bubble curvature of the Richtmyer-Meshkkov instability [15], which is a shock-accelerated interfacial instability. In the Richtmyer-Meshkkov instability, it has been known that the asymptotic bubble curvature is dependent on the density jump [8].

The present models may not be directly applicable to the spike evolution, except the cases of $A \approx 1$. It is because for a finite density jump, the mushroom-like vortex structure is pronounced around the spike, which makes increase of the drag, and therefore this effect should be considered in the modeling. So far, no model for the spike evolution of the finite density jump has been established. Extension of the present models to the spike would be an interesting and challenging subject.

ACKNOWLEDGMENTS

This research was supported by Basic Science Research Program through the National Research Foundation of Korea (NRF) funded by the Ministry of Education, Science and Technology (Grant No. 2012-0002995).

REFERENCES

[1] Lord Rayleigh, *Investigation of the character of the equilibrium of an incompressible heavy fluid of variable density*, Proc. London Math. Soc. **14** (1883), 170–177.
[2] G. I. Taylor, *The instability of liquid surfaces when accelerated in a direction perpendicular to their planes I*, Proc. R. Soc. London A **201** (1950), 192–196.
[3] D. Sharp, *An overview of Rayleigh-Taylor instability*, Physica D **12** (1984), 3–10.
[4] D. Layzer, *On the instability of superimposed fluids in a gravitational field*, Astrophys. J. **122** (1955), 1–12.
[5] J. Zufiria, *Bubble competition in Rayleigh-Taylor instability*, Phys. Fluids **31** (1988), 440–446.
[6] J. Hecht, U. Alon and D. Shvarts, *Potential flow models of Rayleigh-Taylor and Richtmyer-Meshkov bubble fronts*, Phys. Fluids **6** (1994), 4019–4030.
[7] V. N. Goncharov, *Analytic model of nonlinear, single-mode, classical Rayleigh-Taylor instability at arbitrary Atwood numbers*, Phys. Rev. Lett. **88** (2002), 134502: 1–4.
[8] S.-I. Sohn, *Density dependence of a Zufiria-type model for Rayleigh-Taylor and Richtmyer-Meshkov bubble fronts*, Phys. Rev. E **70** (2004), 045301: 1–4.
[9] S.-I. Sohn, *Bubble interaction model for hydrodynamic unstable mixing*, Phys. Rev. E **70** (2007), 066312: 1–12.
[10] S.-I. Sohn, *Effects of surface tension and viscosity on the growth rates of Rayleigh-Taylor and Richtmyer-Meshkov instabilities*, Phys. Rev. E **80** (2009), 055302: 1–4.
[11] Y. G. Cao, H. Z. Guo, Z. F. Zhang, Z. H. Sun and W. K. Chow, *Effects of viscosity on the growth of Rayleigh-Taylor instability*, J. Phys. A: Math. Theor. **44** (2011), 275501: 1–8.
[12] B. Cheng, J. Glimm and D. H. Sharp, *A three-dimensional renormalization group bubble merger model for Rayleigh-Taylor mixing*, Chaos **12** (2002), 267–274.
[13] S.-I. Sohn, *Vortex model and simulations for Rayleigh-Taylor and Richtmyer-Meshkov instabilities*, Phys. Rev. E **69** (2004), 036703: 1–11.
[14] P. Ramaprabhu and G. Dimonte, *Single-mode dynamics of the Rayleigh-Taylor instability at any density ratio*, Phys. Rev. E **71** (2005), 036314: 1–9.
[15] R. D. Richtmyer, *Taylor instability in shock acceleration of compressible fluids*, Commun. Pure Appl. Math. **13** (1960), 297–319.